

Experimentally constrained molecular relaxation: The case of glassy GeSe₂

Parthapratim Biswas,* De Nyago Tafen,[†] and D. A. Drabold[‡]
Department of Physics and Astronomy, Ohio University, Athens, Ohio 45701, USA
 (Received 15 September 2004; published 24 February 2005)

An ideal atomistic model of a disordered material should contradict no experiments, and should also be consistent with accurate force fields (either *ab initio* or empirical). We make significant progress toward jointly satisfying *both* of these criteria using a hybrid reverse Monte Carlo approach in conjunction with approximate first-principles molecular dynamics. We illustrate the method by studying the complex binary glassy material *g*-GeSe₂. By constraining the model to agree with partial structure factors and *ab initio* simulation, we obtain a 647-atom model in close agreement with experiment, including the first sharp diffraction peak in the static structure factor. We compute the electronic state densities and compare to photoelectron spectroscopies. The approach is general and flexible.

DOI: 10.1103/PhysRevB.71.054204

PACS number(s): 61.43.Fs, 71.23.An, 71.15.Mb, 71.23.Cq

I. INTRODUCTION

The modeling of complex materials based upon molecular dynamics (MD) simulation has been one of the remarkable advances in theoretical condensed matter physics. Whether the potentials chosen are empirical or *ab initio*, remarkable insights have accrued for diverse problems in materials physics and beyond. There is, however, an unsatisfying point to the logic of MD simulation: it does not make use of all the information available about a material under study—notably the information implied by experiments. Simulations often cannot achieve agreement with experiment because of short simulation times, small system sizes or inaccuracies in the interactions. Successful prediction of *new* properties is more likely for models in agreement with existing data. Imposition of experimental information may be important in phase-separated or other complex materials for which obtaining a suitable starting structure may be difficult, and for which short MD time scales preclude the emergence of such structures in the model.

A different approach to model construction implemented by McGreevy¹⁻⁴ and colleagues is the so-called “reverse Monte carlo” (RMC) method. Here, one explicitly sets out to make an atomistic model which agrees with experiments. RMC has been widely used to model a variety of complex disordered materials. This is accomplished by making Monte Carlo moves which drive a structural model toward exact agreement with one or more experiments. In practice, RMC is the ideal method to explore the *range* of configurations which are consistent with experiment(s). Without adequate limitation to a “physical” subspace of configuration space, it is unlikely to produce a satisfactory model. That is, only a subset of RMC models [which match the experiment(s)] is physically realistic (consistent with accurate interatomic interactions). The imposition of topological/chemical bonding constraints in RMC can ameliorate this problem, but not remove it entirely.⁵ The mathematical structure of constrained RMC is a constrained optimization “traveling salesman” problem. In our previous implementation of constrained RMC we formed a positive definite (quadratic) cost or “penalty” function ξ , which was then minimized (ideally, but not practically) to zero for a structural model which exactly satisfies all constraints imposed:

$$\xi = \sum_{j=1}^K \sum_{i=1}^{M_j} \eta_i^j \{F_E^j(Q_i) - F_c^j(Q_i)\}^2 + \sum_{l=1}^L \lambda_l P_l, \quad (1)$$

where η_i^j is related to the uncertainty associated with the experimental data points, K is the number of experimental data sets employed, M_K is the number of data for the K th set, and L is the number of additional (nonexperimental) constraints included. The quantity Q is the appropriate generalized variable associated with experimental data $F(Q)$ and $P_l > 0$ is the penalty function associated with each additional constraint with the property that $P_l = 0$ if constraint l is exactly satisfied, and $\lambda_l > 0$. Such “additional” constraints can be of many different forms (for example, one may impose chemical or topological ordering, or phase separated units within a continuous random network) The coordinates of atoms are changed according to Monte Carlo moves, which is akin to a simulated annealing minimization of our cost function ξ . The method is easy to implement, though care must be taken to include the minimum number of independent constraints possible to reduce the likelihood of getting “stuck” in spurious minima. We have shown that inclusion of suitable constraints leads to models of *a*-Si much improved compared to RMC models using only the structure factor [first term of Eq. (1)] as a constraint.⁵

As the creation of models of complex materials is a difficult task, it is of obvious advantage to incorporate *all* possible information in fabricating the model. We assert that an ideal model of a complex material should (1) be a minimum (metastable or global) of a suitable energy functional faithfully reproducing the structural energetics, (2) should contradict no experiments. When stated in these terms, our criterion seems quite obvious, yet current simulation schemes do not simultaneously accommodate both criteria, but focus only on one or the other.

In this paper, we merge the power of *ab initio* molecular simulation with the *a priori* information of experiments to create models consistent with experiments and the chemistry implied by accurate interatomic interactions. To obtain joint agreement, we unite MD with the reverse Monte Carlo (RMC) method. We name the scheme “experimentally constrained molecular relaxation” (ECMR). One can understand

our scheme as a way to “tune” a structural model using MD within the space of *experimentally realistic* models as defined by RMC. We choose a troublesome and complex material with a long experimental and modeling history: g -GeSe₂.

From an algorithmic perspective, our scheme has important advantages. For example, to model a glass such as GeSe₂ or SiO₂ using first-principles methods, the method of choice is to form an equilibrated liquid, use some dissipative dynamics to simulate an (unphysically) rapid quench of the liquid into an arrested phase and finally to relax this to a local energy minimum, presumably at astronomical fictive temperature (high potential energy). Usually some repeated “annealing” cycles are also used. If one is interested in a glassy phase all the work of forming and equilibrating the liquid is redundant, and it is a pious hope that the arrested liquid will resemble a real glassy phase. Evidently the likelihood for success is strongly affected by topological and chemical similarity of the melt to the physical amorphous phase. If complex ordering “self-organization” or phase separation occurs in the physical amorphous phase, the short simulations of conventional *ab initio* schemes will surely miss these important structural features. In this vein, we have used ECMR to construct models of α -Si with intermediate range order on a nanometer length scale⁶ by inclusion of fluctuation electron microscopy.⁷ We note that successful techniques do exist to tackle the time-scale problem,^{8,9} though these do not enable the inclusion of experimental information. Our method is efficient enough to enable the creation of a 647 atom model of g -GeSe₂ using only a workstation. The method is at least a factor of five faster than a comparable quench from the melt simulation, with its inherent limitations.

II. METHOD

The obvious means to incorporate interatomic interactions into an RMC simulation is to add a constraint to minimize the magnitude of the force on all the atoms according to some energy functional or to minimize the total energy. For an *ab initio* Hamiltonian this is expensive, since Monte Carlo minimization of Eq. (1) requires a large number of energy/force calls. Thus, we have instead employed a simple “self consistent” iteration scheme (indicated in Fig. 1): (1) starting with an initial configuration C_1 , minimize ξ to get C_2 , (2) steepest-descent quench C_2 with an *ab initio* method to get C_3 , (3) subject the resulting configuration to another RMC run (minimize ξ again), repeat steps (2) and (3) until both the MD relaxed model and RMC models no longer change with further iteration. In this paper, we limit ourselves to the first term in Eq. (1) (the experimental static structure factor), though additional constraints (experimental or other) certainly could be employed. For the RMC component of the iteration, we make the conventional choice of using Monte Carlo for the minimization. This is simple and does not require gradients [and thus allows the use of nonanalytic terms in Eq. (1) (Ref. 10), if desired].

We emphasize that our method is *flexible*. Its logic suggests that one should include whatever experimental infor-

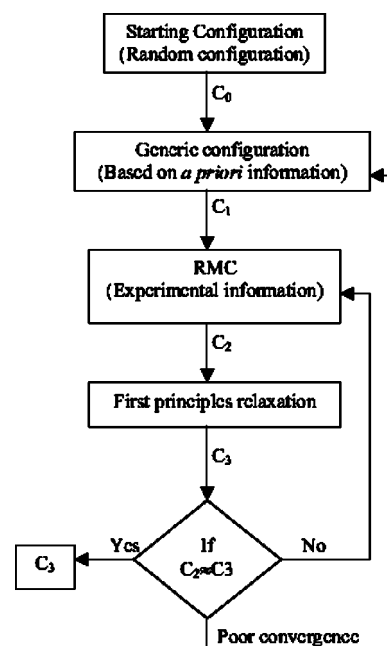


FIG. 1. Flow diagram for the “experimentally constrained molecular relaxation” method of this paper.

mation is available. These might be costly to include (for example, to compel agreement with the vibrational density of states, the dynamical matrix would be required at each iteration). The method is equally suited to fast empirical potentials, which would allow studies of very large models. It is also possible to force a close fit to some restricted range of data, and a less precise fit elsewhere if desired. Our scheme also provides insight into the topological signatures of different constraints (experimental or otherwise). Chemical and or topological constraints could also be maintained as part of the RMC iteration.

Our method can be understood as a way to minimize an effective potential energy function $V_{\text{eff}}(R) = V(R) + \Lambda \zeta(R)$, where $V(R)$ is the potential energy of the configuration (denoted by R), $\Lambda > 0$, and ζ is a non-negative cost function enforcing experimental (or other) constraints as in Eq. (1). Empirically, we find that it is possible to find configurations that simultaneously approximately minimize both terms (which implies that the choice of Λ is not very important). It is also clear that our method is really *statistical*: in general, one should generate an ensemble of conformations using ECMR. For adequately large models, self-averaging can be expected; in this study of large (647 atom) models of g -GeSe₂ we find similar results for two runs; for small systems a proper ensemble average is required.

This method needs to be studied and developed in a number of ways. Nevertheless, we show in this paper that it is relatively easy to model a particularly challenging material with significant advantages in both experimental plausibility of the model and computational efficiency of the algorithm.

III. APPLICATION TO GLASSY GeSe₂

We apply ECMR to glassy GeSe₂, a classic glass forming material with challenging physical and technical issues: (1) it

TABLE I. The convergence of ECMR described in the text.

ECMR iteration	Average force/atom (eV/Å)
1	2.242×10^{-3}
2	7.365×10^{-3}
3	6.518×10^{-4}
4	5.019×10^{-4}
5	4.773×10^{-4}
6	4.903×10^{-4}
7	4.686×10^{-4}
8	4.642×10^{-4}

displays nanoscale order: a “first sharp diffraction peak” (FSDP) is observed in neutron diffraction measurement, (2) the packing of GeSe tetrahedra involves both edge- and corner-sharing topologies, (3) the material has interesting photoresponse (understanding of which requires the electronic structure), (4) the material is difficult to simulate with *ab initio* techniques.^{11–14} The model used in our calculation consists of 647 atoms in a cubic box of size 27.525 Å.

In the nomenclature of Fig. 1, C_1 is obtained by constraining the coordination number (2 for Se, 4 for Ge) and the bond-angle distribution of Se-Ge-Se to an approximate Gaussian with an average bond angle 109.5°. The initial network was “generic” and included none of the detailed local chemistry of Ge and Se aside from the coordination and chemical ordering (bond angles were not constrained in RMC loops). Equal weighting was used for all experimental points in this paper. Using the method of isotopic substitution, Salmon and Petri¹⁵ were able to separately measure the three (Ge-Se, Ge-Ge, and Se-Se) partial structure factors of g -GeSe₂. We jointly enforced all three partials (in real space) in the RMC component of the loop in Fig. 1. The MD relaxation was done with FIREBALL.¹⁶ It was found that after the fourth iteration, $S(Q)$ hardly changed. In Table I, we show the average force per atom at the beginning of each call to MD relaxation; good convergence is observed. Subsequent discussion in this paper is for the last step of the MD, with forces less than 1×10^{-2} eV/Å. It was not obvious to us in the beginning that RMC and first principles interatomic interactions could be made “self-consistent,” but for this system at least, reasonable convergence is possible. It is likely that some initial conformations C_1 will get “stuck” and require a new start.

A. Structure

In Fig. 2, we compare the RMC, ECMR, and experimental structure factors. Here, the RMC model is that obtained by starting with the generic C_0 configuration, and forcing agreement on the experimental $S(Q)$ (without any other constraints). While the agreement is very good, it is not perfect. This is to be expected for three reasons: (1) consistency between data and Hamiltonian is never exact, (2) our cell contains 647 atoms, which is compared to the thermodynamic limit, and (3) we chose to constrain our model using real space data, which involves Fourier transforms and window-

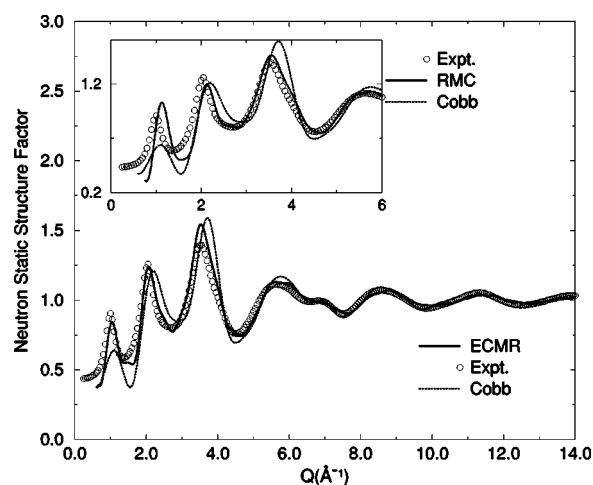


FIG. 2. Neutron-weighted static structure factor, comparing ECMR model, experiment (Ref. 15) and a quench from the melt made with the same Hamiltonian used with ECMR (Ref. 13). Inset: blowup of the small- Q region showing initial RMC model (e.g., enforcing experimental structure factor, but without ECMR iterations), experiment (Ref. 15), and quench from the melt model due to Cobb *et al.* (Refs. 13 and 14). The first sharp diffraction peak is closely reproduced by ECMR and RMC, and is present but weak in the quenched model.

ing (this introduces only small errors in this data set). In Fig. 2 we highlight the differences between experiment,¹⁵ a quench from the melt model¹³ and the new ECMR model. In the inset of Fig. 2, we also illustrate the level of agreement using a pure RMC approach, which is similar to the ECMR result and notably better than quench from the melt. For reference, we have reproduced the full partial structure factors elsewhere.⁶

Note in Fig. 2 that the first sharp diffraction peak (FSDP) is well reproduced, (very close in width and centering, and much improved from all previous models in height). Moreover, as for our “decorate and relax” (DR) method,¹⁷ the large Q structure closely tracks experiment (unlike the experience for quench from the melt models which are too liquidlike and therefore decay too rapidly for large Q). These desirable features are of course “built in;” we show here that the ECMR method does preserve every important feature of the structure of the glass manifested in $S(Q)$.

An important indicator of network topology and medium range order of GeSe₂ glass is the presence of edge-sharing and corner-sharing tetrahedra. Raman spectroscopy¹⁸ and neutron diffraction¹⁹ studies have indicated that 33 to 40 % of Ge atoms are involved in edge sharing tetrahedra. The fraction in our model is found to be 38%. This was not “built in” to our modeling, and is a pleasing prediction arising from the procedure. We also have observed that 81% of Ge atoms in our model are fourfold coordinated of which approximately 75% form predominant Ge-centered structural motifs Ge(Se_{1/2})₄ while 6% are ethanelike Ge₂(Se_{1/2})₆ units. The remaining Ge atoms are threefold coordinated and are mostly found to be bonded as Ge-Se₃ units. On the other hand, the percentage of twofold, threefold, and onefold coordinated Se

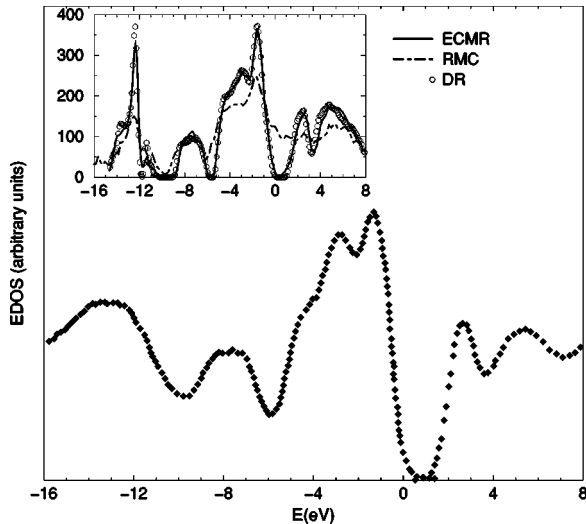


FIG. 3. The electronic density of states (Gaussian-broadened Kohn-Sham eigenvalues) for ECMR model of GeSe_2 , along with the RMC model (not using *ab initio* information) and a “decorate and relax” (DR) model made with the same Hamiltonian (inset). The XPS (Ref. 21) and IPES (Ref. 22) data show the occupied (valence band) and unoccupied (conduction band) part of the spectrum. See Table II for numerical comparison of the peaks. The Fermi level is at $E=0$. Both DR and ECMR reproduce the state density closely, while the RMC model lacks an optical gap.

atoms are 72, 18, and 10 %, respectively. Mössbauer experiments, where Sn was used as a Ge probe,²⁰ estimated that the fraction of Ge involved in dimers is 16% which is again in favor of our model.

By integrating partial radial distribution functions via Fourier transform of structure factors Petri and Salmon¹⁵ obtained nearest-neighbor coordination numbers $n_{\text{Ge-Ge}}=0.25$, $n_{\text{Se-Se}}=0.20$, and $n_{\text{Ge-Se}}=3.7$ that corresponds to average coordination number $\bar{n}=2.68$. The corresponding values from our model are $n_{\text{Ge-Ge}}=0.17$, $n_{\text{Se-Se}}=0.30$, $n_{\text{Ge-Se}}=3.68$, and $\bar{n}=2.66$. The partial and total coordination numbers, therefore, agree well with experiments (as expected) and are consistent with the 8-*N* rule which predicts $\bar{n}=2.67$. The percentage of homopolar bonds present in our model is found to be about 6.2% which is again very close to the value 8% noted by Petri and Salmon.¹⁵

B. Electronic density of states

Having studied structural properties, we now briefly analyze electronic properties of our model. Since structural and electronic properties are intimately related, an examination of electronic density of states provides an additional test of the validity of the model which is derived jointly from structural information and a suitable interatomic interaction. The electronic density of states (EDOS) is obtained by convolving each energy eigenvalue with suitably broadened Gaussian. The ECMR EDOS in the inset of Fig. 3 agrees quite well with experimental results obtained from x-ray photoemission²¹ (XPS), inverse photoemission spectroscopy²² (IPES), and ultraviolet photoemission spectroscopy²³ (UPS) measurements as well as with those obtained in recent

TABLE II. The positions of the A_1 , A_2 , A_3 , and B peaks in the EDOS of GeSe_2 glass compared to experimental results (Ref. 23).

(eV)	A_1	A_2	A_3	B
Present work	-1.55	-3.0	-4.6	-7.4
Experiment (Ref. 23)	-1.38	-3.0	-4.6	-7.8
Melt and quench (Ref. 13)	-1.4	-2.7	-4.6	-7.0
Decorate and relax (Ref. 12)	-1.36	-2.8	-4.5	-7.2

theoretical studies.^{12,13,24,25} It is remarkable that the Kohn-Sham eigenvalues (obtained in the Harris approximation) agree so well with the photoelectron spectroscopy,²⁶ particularly as the energy-dependent matrix element is not included in the calculation. The substantial splitting between the first two peaks of the valence bands named the A_1 and A_2 peaks is also well pronounced. The position of the principal peaks obtained from the different models and experiment are tabulated in Table II. The similarity of experiment and theory suggests the utility of a study of the Kohn-Sham eigenvectors to enable atomistic identification of defects and bands illustrated in Fig. 3.

We also compare the EDOS for the RMC model. The RMC model does very poorly, without even showing an optical gap, despite the excellent static structure factor (obtained by construction). By contrast, our DR and the quench from the melt model (not shown) are very close to experiment and ECMR. As the coordination and chemical order is correct in the RMC model, the lack of an optical gap originates in an unrealistic bond angle distribution in the RMC model [something very similar happens in *a*-Si if only $S(q)$ (and no bond angle constraint) is used to form the model⁵]. This result emphasizes the need to compute the density of electron states as an important gauge of the credibility of a model.

C. Vibrations

It is useful to also examine the vibrational density of states (VDOS) of our ECMR model due to the close relation-

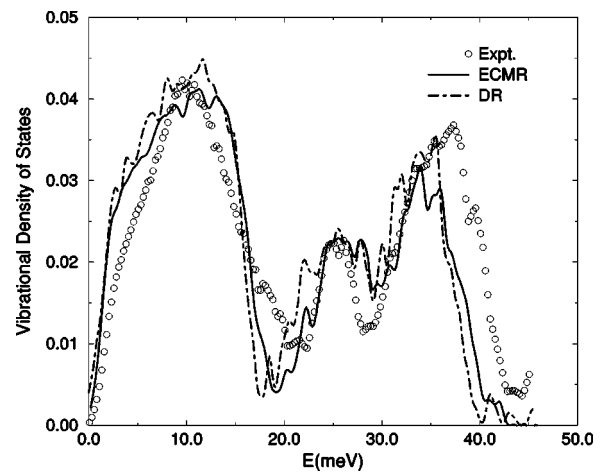


FIG. 4. Vibrational density of states computed from dynamical matrix for 648 atom models and experiment (Ref. 27).

ship to its atomic-scale structure and its dynamical properties. The VDOS was reported elsewhere.¹³ Comparing our VDOS with experiment obtained by inelastic neutron scattering,²⁷ the spectrum exhibits the same features with somewhat better resolution than results we reported in Ref. 13. Three bands can be distinguished: a low-energy acoustic band involving mainly extended interblock vibrations and a high-energy optic band consisting of more localized intrablock vibrations. The two main bands are clearly separated by the tetrahedral breathing (A_1 - A_{1c}) band. The overall agreement is quite reasonable, including a resolved A_1 “companion” mode “ A_{1c} .”

In Fig. 4, we compare the vibrational density of states of the ECMR model with experiment²⁷ and for completeness our decorate and relax model including 648 atoms along with the ECMR model. We do not present the RMC result, as the system is not at equilibrium according to FIREBALL, which would therefore lead to many imaginary frequencies in the density of states. While generally DR and ECMR are quite similar, we note some difference in the tetrahedral breathing A_1 band (near 25 meV), including a slightly different

A_1 - A_{1c} splitting. This is probably because the ratio of edge to corner sharing tetrahedra is different ($\approx 29\%$ of Ge atoms are involved in edge sharing tetrahedra in the DR model). This suggests that the VDOS has some sensitivity to medium range order (tetrahedral packing) in this glass.

IV. CONCLUSION

In summary, we have proposed a method which enables the inclusion of *a priori* information (experimental or otherwise) into molecular simulation. We have shown that the method is effective for a challenging material g -GeSe₂.

ACKNOWLEDGMENTS

We thank Dr. P.S. Salmon for providing us with experimental data, Professor Himanshu Jain, and Professor John Abelson for helpful discussions. We acknowledge the support of National Science Foundation for support under Grants Nos. DMR-0074624, DMR-0205858, and DMR-0310933.

*Electronic address: biswas@phy.ohiou.edu

†Electronic address: tafende@helios.phy.ohiou.edu

‡Electronic address: drabold@ohio.edu

¹O. Gereben and L. Pusztai, Phys. Rev. B **50**, 14 136 (1994).

²J. K. Walters and R. J. Newport, Phys. Rev. B **53**, 2405 (1996).

³R. L. McGreevy, J. Phys.: Condens. Matter **13**, R877 (2001).

⁴R. L. McGreevy and L. Pusztai, Mol. Simul. **1**, 359 (1988).

⁵P. Biswas, R. Atta-Fynn, and D. A. Drabold, Phys. Rev. B **69**, 195207 (2004).

⁶P. Biswas, D. N. Tafen, R. Atta-Fynn, and D. A. Drabold, J. Phys.: Condens. Matter **16**, S5173 (2004).

⁷M. M. J. Treacy and J. M. Gibson, Acta Crystallogr., Sect. A: Found. Crystallogr. **52**, 212 (1996).

⁸See for example, G. T. Barkema, and N. Mousseau, Phys. Rev. B **62**, 4985 (2000), and references therein.

⁹G. Henkelman and H. Jonsson, J. Chem. Phys. **113**, 9978 (2000); G. Henkelman, B. P. Uberuaga, and H. Jonsson, *ibid.* **113**, 9901 (2000).

¹⁰It is possible that suitable gradient-based methods could provide more rapid convergence, a point we do not investigate here.

¹¹C. Massobrio, A. Pasquarello, and R. Car, Phys. Rev. Lett. **80**, 2342 (1998).

¹²D. N. Tafen and D. A. Drabold, Phys. Rev. B **68**, 165208 (2003).

¹³M. Cobb, D. A. Drabold, and R. L. Cappelletti, Phys. Rev. B **54**, 12 162 (1996).

¹⁴X. Zhang and D. A. Drabold, Phys. Rev. B **62**, 15695 (2000).

¹⁵I. Petri, P. S. Salmon, and H. E. Fische, Phys. Rev. Lett. **84**, 2413

(2000).

¹⁶O. F. Sankey and D. J. Niklewski, Phys. Rev. B **40**, 3979 (1989); O. F. Sankey, D. A. Drabold, and G. B. Adams, Bull. Am. Phys. Soc. **36**, 924 (1991).

¹⁷D. A. Drabold, Jun Li, and D. N. Tafen, J. Phys.: Condens. Matter **15**, S1529 (2003).

¹⁸K. Jackson, A. Briley, S. Grossman, D. V. Porezag, and M. R. Pederson, Phys. Rev. B **60**, R14 985 (1999).

¹⁹S. Susman, K. J. Volin, D. G. Montague, and D. L. Price, J. Non-Cryst. Solids **125**, 168 (1990).

²⁰P. Boolchand, J. Grothaus, W. J. Bresser, and P. Suranyi, Phys. Rev. B **25**, 2975 (1982).

²¹E. Bergignat, G. Hollinger, H. Chermette, P. Pertosa, D. Lohez, M. Lannoo, and M. Bensoussan, Phys. Rev. B **37**, 4506 (1988).

²²S. Hosokawa, Y. Hari, I. Ono, K. Nishihara, M. Taniguchi, O. Matsuda, and K. Murase, J. Phys.: Condens. Matter **6**, L207 (1994).

²³S. Hino, T. Takaharshi, and Y. Harada, Solid State Commun. **35**, 379 (1980).

²⁴S. G. Louie, Phys. Rev. B **26**, 5993 (1982).

²⁵W. Pollard, J. Non-Cryst. Solids **144**, 70 (1992).

²⁶R. M. Martin, *Electronic Structure, Basic Theory and Practical Methods* (Cambridge University Press, Cambridge, 2004), p. 144.

²⁷R. L. Cappelletti, M. Cobb, D. A. Drabold, and W. A. Kamitakahara, Phys. Rev. B **52**, 9133 (1995).